CHAPTER 6

SUMMARY AND OUTLOOK

§6.1 SUMMARY

MANY DEFORMATION processes take place at high rates, for instance a metal plate that is blown into shape by an explosion, or a bullet penetrating an armour plate. Even less violent processes with a low *global* strain rate sometimes exhibit *local* strain rates of 10^3–10^4 s^{-1}. One example is punching a hole into a metal plate. Under such violent conditions, it is very difficult to determine experimentally the mechanical response *during* the deformation. Nevertheless, there exists a strong interest in industry to be able to predict the deformation under these extreme conditions. Accurate predictions during the design phase may eliminate processing steps afterwards. Currently, many of these predictions are based on material behaviour that is *supposed* to be known on a *macroscopic* scale, the so-called *constitutive equations*.

In this thesis, a different approach is proposed: predict the *macroscopic* properties based on *microscopic* processes. A certain line defect in a polycrystalline material, the so-called *dislocation*, is considered as a singular dogsbody of the mechanical load. Specifically, the research focuses on the shear deformation of a single grain on the micrometer scale. At this length scale, the stresses and displacements of dislocations play an important role, as well as their mutual interactions and their interactions with obstacles.

After a historical overview in Chapter 1 the methodology of the simulations is described in Chapter 2. The modelling is executed in a two-dimensional computational cell that is periodic in the horizontal direction. The computational cell represents a slip system in one grain of a close-packed metal. To that end, the computational cell contains edge dislocations moving on parallel, horizontal slip planes. Furthermore, the slip plane contains areas where dislocations are generated, and obstacles that sometimes block the motion of dislocations. Rules are implemented for the case of meeting of two dislocations.

The deformation of the computational cell is calculated using the method of Discrete Dislocation Plasticity (DDP). This method has been chosen because it describes explicitly the dislocation-dislocation interactions and takes the effects of the boundaries explicitly into account. The stress- and displacement fields of edge dislocations in an *infinite* medium are well known. In the case of a *finite* medium the boundaries may have an important contribution. The DDP-method solves this by splitting the problem. First, the interactions of dislocations are described as if they were in an infinite medium. Next, the fields are corrected for the effects of the boundaries using a finite-element method.

In extreme cases, the dislocation moves at velocities comparable to the velocity of sound in the material. In an elastic description, the velocity of sound is the maximum attainable signal velocity. At those velocities, the stresses and displacements of a dislocation can no longer be approximated by their static form. In order to describe the fields at high dislocation velocities, a Lorentz transformation has to be applied. In this case, the velocity of sounds takes the role of the speed of light in special relativity. Especially for high velocities, the field changes drastically: at the slip plane the sign of the shear stress may even reverse!

When the stress exceeds a certain value, the obstacles are no longer able to block the dislocation motion, although the dislocation motion is still damped. This is called the viscous regime. Chapter 3 considers the physical mechanisms that play a role. The relation between the stress and the dislocation velocity is called the *drag-relation*. Usually a linear relation is assumed. However, this would lead to supersonic dislocation velocities at high stresses. By considering different physical damping mechanisms (pinning by impurities, electron and phonon drag) we *derived* a drag relation which is very similar to the *postulated* relation in literature. The mechanism of pinning by a cloud of impurities, which is a dominant mechanism at slow deformation, turns out to be ineffective already at very low dislocation velocities.

The simulations of Chapter 4 show that some dislocations do indeed reach the velocities at which the fields change significantly. This causes large differences in the displacements and stresses *locally*. Nevertheless, a comparison of the stress-strain curves at a higher length scale shows that this does *not* influence them significantly. The reason for this is that relatively only a few dislocations actually

reach the high velocities, and that the local stress peaks are averaged out over the top- and bottom planes when the stress-strain curve is calculated. On the other hand, at strain rates of the order of 10^6 s^{-1}, inertial effects become important and may no longer be neglected.

One of the effects of a very fast local deformation is a sudden temperature rise. Chapter 5 deals with this. The temperature rise may be so high as to cause local melting of the material. The temperature rise is caused by mechanical work being converted into heat. Due to the short processing time, the generated heat has not enough time to spread through the material. Locally, this causes a very high temperature rise. In turn, the obstacle strengths are effectively lowered and the dislocation damping becomes stronger. This causes the deformation to be a different one from the case where the heat has had enough time to spread over a larger volume.

Some estimates exist in the literature of the magnitude of the temperature rise caused by moving dislocations. These analyses hold for thermal equilibrium, low deformation rates and a constant distance between the dislocations. It follows from these analyses that the maximum temperature rise by moving dislocations is of the order of some *tens* of degrees, which is not enough by far to induce melting. One explanation for the melting is the sudden release of a dislocation pile-up against an obstacle. All energy that is stored in the pile-up could be converted into heat during a very short time.

Chapter 5 addresses the question whether these conclusions also hold for fast deformations. The method of DDP has the advantage that the positions and velocities of all heat sources (the dislocations) are known, and is therefore very useful to predict the temperature rise exactly. Chapter 5 shows that the temperature field may be calculated analytically as well as numerically, taking into account the fact that the processing time is shorter than the time needed by the generated heat to attain an equilibrium distribution. The analytical model is then used to validate the numerical model. The model shows the localisation of the temperature rise in Aluminium and in Titanium. Even at a strain rate of 10^6 s^{-1}, the temperature rise due the moving dislocations is at most a few tens of degrees, thereby confirming the earlier estimates.

This Chapter 6 contains also an outlook. The result of the temperature rise due to ordinary plastic flow, as predicted in Chapter 5 with the DDP-method, is compared to the results obtained from the constitutive equation. This prediction contrasts with the experimental result of melting. It is suggested that the experimentally observed temperature rise may be caused by crack propagation. The stresses and displacements around a crack can be described in terms of pile-ups of dislocations. This, in turn, can be modelled within the framework of DDP including full dynamic, i.e. inertia effects and pre-existing dislocations around the crack. So far we may conclude that the local temperature rise due to fast deformation is only

for a small part due to the ordinary plastic flow, while the dissipation due to a moving crack may heat up the material with hundreds of degrees depending on the thermo-physical properties.

§6.2 DISCUSSION AND OUTLOOK

In the next section, some of the results from the previous chapters are discussed. A comparison is made between the macroscopic description of plastic deformation and the mesoscopic approach based on the discrete dislocation plasticity model. The connection between dislocations, cracks and the temperature rise is considered, leading to the outlook in section 6.3, dealing with fracture dynamics in the framework of discrete dislocation plasticity. However, first the conclusion of chapter 4 that accelerations take place at the picosecond timescale is discussed.

6.2.1 ACCELERATIONS

In Chapter 4 it was shown that the time interval needed for a dislocation to reach, say, 90% of its final velocity is of the order of a picosecond if a high resolved shear stress is active (μ/30). A few tens of picoseconds are needed if a much lower load is applied (μ/1000). To check consistency with the *macroscopic* description we return to Chapter 3. The macroscopic formulation of the acceleration as a function of the dislocation velocity can readily be obtained from the equations in section 3.4. Assuming a straight dislocation, equation (3.4–1) can be rewritten as:

$$\rho b^2 v_{\mathrm{DIS}}^2 a_2 \left(a_2^2 - v_{\mathrm{DIS}}^2\right)^{-3/2} a + \rho b^2 \left(\frac{a_2^2}{a_2^2 - v_{\mathrm{DIS}}^2}\right)^{1/2} a - b\sigma_{\mathrm{PK}} + \frac{B_0 v_{\mathrm{DIS}}}{1 - v_{\mathrm{DIS}}^2 / a_2^2} = 0 \qquad (6.2\text{–}1)$$

where σ_{PK} represents the acting shear stress and a is the acceleration. If only relativistic effects, i.e. without a drag term, are considered, the acceleration from zero initial velocity would steadily decrease to zero. However, the involvement of the drag term appears to have a substantial effect. In figure 6.2–1 the acceleration is plotted as a function of the velocity and it shows that, provided drag is included, a steady state is reached already around $0.25a_2$ at a resolved shear stress σ_{PK} of μ/1000 (left figure). If σ_{PK} is much larger, say μ/30 (as in section 4.3) the acceleration goes to zero at a much higher value for the velocity, i.e. around 95% of the shear wave velocity (right figure 6.2–1). In the former case steady state is attained in about 0.5 ns and in about 5 ps if a very high shear stress is active. Indeed, about the same value was found based on the discrete dislocation plasticity approach (figure 4.3–2) for both stress levels.

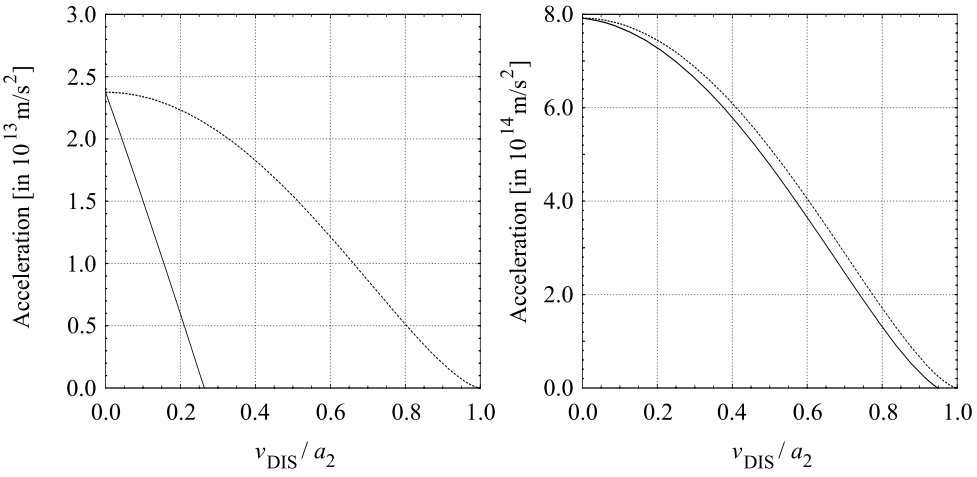

FIGURE 6.2–1 Acceleration of a straight dislocation in Cu (for material properties see table 4.1–1 on page 60). The solid lines include drag; the dashed lines do not. Left $\sigma_{PK} = \mu/1000$, right $\sigma_{PK} = \mu/30$.

In general, it can be concluded that the acceleration is extremely high and the time needed to bring the dislocation to a steady state velocity is very short. The dislocation will reach steady state velocity after it has travelled over a very small distance, i.e. about l% or even less of its mean slip distance. Consequently, the time interval and distance required to bring the dislocation to its steady-state situation is so small that in a *physical* description it can be neglected. This is in agreement with the conclusions by Gillis and Kratochvil[1].

6.2.2 TEMPERATURE RISE AND CRACKS

Another point for a comparison between a macroscopic description and the DDP approach concerns the temperature rise due to plastic deformation. The temperature rise based on DDP was predicted in Chapter 5: at a shear strain of 7% the temperature rises with about 10 – 20 K in Al and Ti. Macroscopically, in a homogeneously strained material the temperature rise induced by mechanical work up to a certain strain γ_F can simply be equated to

$$\Delta T = \frac{\xi}{\rho c_P} \int_0^{\gamma_F} \tau \, \mathrm{d}\gamma \tag{6.2–2}$$

where ξ is the fraction of mechanical work converted into heat, ρ the material density and c_P the specific heat at constant pressure. Substitution of the constitutive equation proposed by Johnson et al.[2] (equation (3.1–5)) leads (for $m = 1$ and B and C constants) to

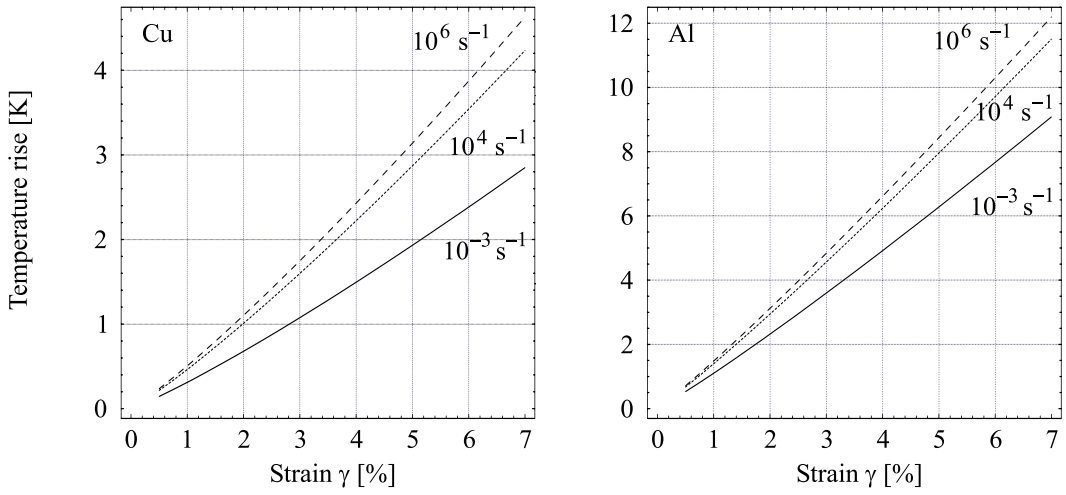

FIGURE 6.2–2 Temperature rise in Cu (left) and Al (right) according to equation (6.2–3), for different strain rates. In both cases, T_R = 300 K, $\dot{\gamma}_0$ = 1 s^{-1} and ξ = 0.9. For Cu, B = 292 MPa, C = 0.025, τ_0 = 90 MPa and n = 0.31. For Al, B = 426 MPa, C = 0.015, τ_0 = 265 MPa and n = 0.34.

$$\Delta T = \left(T_m - T_R\right)\left\{1 - \exp\left[\frac{-\xi\left(1 + C\ln\left(\frac{\dot{\gamma}}{\dot{\gamma}_0}\right)\right)}{\rho c_P\left(T_m - T_R\right)}\left(\tau_0\gamma_F + \frac{B\gamma_F^{n+1}}{n+1}\right)\right]\right\}. \qquad (6.2–3)$$

With the corresponding physical parameters for Al and Cu the temperature rise as a function of strain is displayed in figures 6.2–2 and 6.2–3, respectively. These are similar to the results from De Andrade et al.[3], although their results are erroneous because of mistakes in the actual strain values. Here, ξ was taken to be 0.9 and the strain rates varies between 10^{-3} and 10^6.

In accordance with the DDP calculations the temperature rise lies in the range of a few degrees, somewhat higher for Al than for Cu but still less than 10 K for high strain rate deformation. Even at a high yield stress τ_0 and deformation at high strain rates (10^4 s^{-1}), the temperature rise is predicted to be around 25 K. Experimentally however, a temperature increase up to the melting point is observed in a Ti-alloy[4]. The order of magnitude of temperature rise as predicted by both the DDP-approach and the calculations based on the constitutive equation, is far too small to explain this melting. This is even so at very high strain rates and stresses. One mechanism that might give the proper order of magnitude is the propagation of a crack. This makes sense, because after all, the molten material is observed on the *fracture* surface of Ti-alloys[4]. In addition, there is a close connection between dislocation pile-ups (as discussed in section 5.1) and cracks, as we will see in the section 6.3.

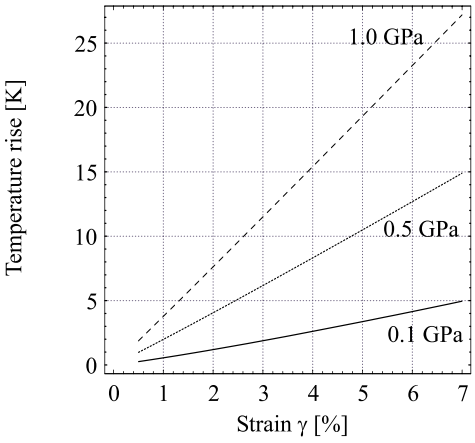

FIGURE 6.2–3 Temperature rise according to equation (6.2–3) in Cu at a *fixed* strain rate $\dot{\gamma} = 10^4\ s^{-1}$. Solid line $\tau_0 = 0.1$ GPa, dotted line $\tau_0 = 0.5$ GPa, dashed line $\tau_0 = 1.0$ GPa. Otherwise, the parameters are the same as in figure 6.2–2.

We start with equation (5.3–4) and the heat source term, $\dot{q}_V(x_1, x_2, t)$, is now the plastic work rate. In the following we assume that the energy dissipation is not uniform in the material, but occurs non-uniformly in a restricted region around the moving crack. Carslaw and Jäger[5] present the general solution of equation (5.3–4) which in this case is converted into

$$\Delta T(x_1, x_2, t) = \frac{1}{4\pi\kappa}\int_0^t \left\{ \iint_{A_P} \frac{\dot{q}_V(\alpha,\beta,t)}{\rho c} \exp\left[-\frac{(x_1-\alpha)^2 + (x_2-\beta)^2}{4\kappa(t-\tau)} \right] \mathrm{d}\alpha\ \mathrm{d}\beta \right\} \frac{\mathrm{d}\tau}{t-\tau}$$

(equation (6.2–4)). The integration in α and in β is taken over the *plastically* deforming region A_P at time t. The coordinates x_1 and x_2 are centred on the moving crack tip. The equation can be used to calculate the temperature field around a stationary crack that is loaded very rapidly. For a *running* crack one may assume that the size of the plastic zone and the crack velocity are constant. Then for heat sources moving at a constant speed, i.e. at a velocity equal to the crack velocity v_{CRACK}, the temperature rise at (x_1, x_2) is

$$\iint_{A_P} \frac{F(\alpha,\beta)}{2\pi\rho} \exp\left[-\frac{v_{CRACK}(x_1-\alpha)}{2\kappa} \right] K_0\left\{ \frac{v_{CRACK}}{2\kappa} \left[(x_1-\alpha)^2 + (x_2-\beta)^2 \right]^{1/2} \right\} \mathrm{d}\alpha\ \mathrm{d}\beta$$

(equation (6.2–5)), where K_0 is the modified Bessel function of the second kind. The functions $\dot{q}_V(x_1, x_2, t)$ and $F(\alpha, \beta)$ depend on the actual plasticity model employed under the assumption that a plastic work rate of $F(\alpha, \beta) = \tau_{ij}\dot{\gamma}_{ij}^{p}$ results. An approximate non-hardening plane strain analysis for small scale yielding predicts[6] the extent of the plastic region as :

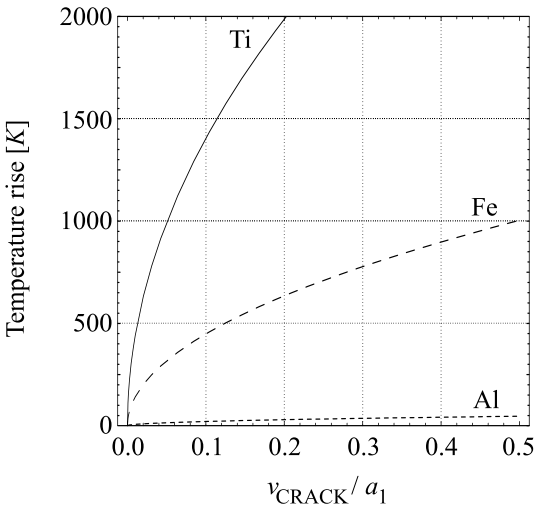

FIGURE 6.2–4 Temperature rise as a function of the crack velocity in Al, Fe and Ti for a Dugdale crack ($K_{\text{cast Al}}$ = 22 MPa m^{½}, $K_{\text{low alloy steel}}$ = 55 MPa m^{½}, $K_{\text{Ti alloy}}$ = 55 MPa m^{½}).

$$R_{\text{P}} = \frac{3(1-\nu)}{\sqrt{2}(2+\pi)}\left(\frac{K}{2\tau_0}\right)^2 \cos(2\theta-\pi) \equiv \omega\cos(2\theta-\pi) \tag{6.2–6}$$

with ν the Poisson's ratio and τ_0 is the yield stress in shear. The associated plastic work rate at points within the plastic zone ($r < R_{\text{P}}$) is[6]

$$\dot{q}_{\text{V}}(\alpha,\beta,t) = \frac{\tau_0^2}{\mu r}\cos(2\theta-\pi)\frac{\text{d}\omega}{\text{d}t}\,. \tag{6.2–7}$$

By substitution of the latter equation into the heat transport equation (6.2–5), the time variation of the heat source term reduces to the time variation of the stress intensity factor.

Another approach is to take Dugdale's description, which represents yielding by viewing the crack as longer by a length, equal to the plastic zone[7]:

$$\omega = \frac{\pi}{8}\left(\frac{K}{\tau_0}\right)^2 \tag{6.2–8}$$

with τ_0 the effective yield stress. Assuming that the plastic zone remains *fixed* in size, i.e. corresponding to the size of the crack as the crack propagates, the work rate is[8]

$$F(\alpha,\beta)=\frac{2(1-\nu)\tau_0^2}{\pi\mu}\ln\left[\frac{1+(1-x_1/\omega)^{1/2}}{1-(1-x_1/\omega)^{1/2}}\right]\delta(\beta)v_{\mathrm{CRACK}}\,, \tag{6.2–9}$$

where $\delta(\beta)$ is the Dirac delta function resulting from the discontinuity in the plastic zone. Substituting the latter equation into $T(x_1, x_2)$ results in a maximum temperature rise of

$$\Delta T_{\max}=\sqrt{2}\,\frac{(1-\nu)K\tau_0\sqrt{v_{\mathrm{CRACK}}}}{2\mu\sqrt{\rho ck}}\ \text{ for }\ \frac{v_{\mathrm{CRACK}}\omega}{2\kappa}\to\infty\,. \tag{6.2–10}$$

with k the thermal conductivity.

This analysis indicates that for a given stress intensity factor the temperature rise is proportional to $(v_{\mathrm{CRACK}})^{1/2}$. The actual value depends also on the yield stress chosen because the increase is proportional to the product of the yield stress and the stress intensity factor. In figure 6.2–4 the temperature rise of various materials is plotted as a function of the normalised crack velocity. The stress intensity factors and the yield stress, all at room temperature, were taken to be constant (from literature). In contrast to the findings of the temperature rise due to dislocation motion, it is striking to see that upon crack propagation a far higher temperature rise is predicted. Equation (6.2–10) also yields a plot of the temperature rise as a function of the stress intensity factor as depicted in figure 6.2–5 (at constant crack velocity of $0.4a_2$).

Although the result is encouraging, several aspects need to be investigated further. In a macroscopic sense, the toughness (i.e. critical stress intensity factor) *in-*

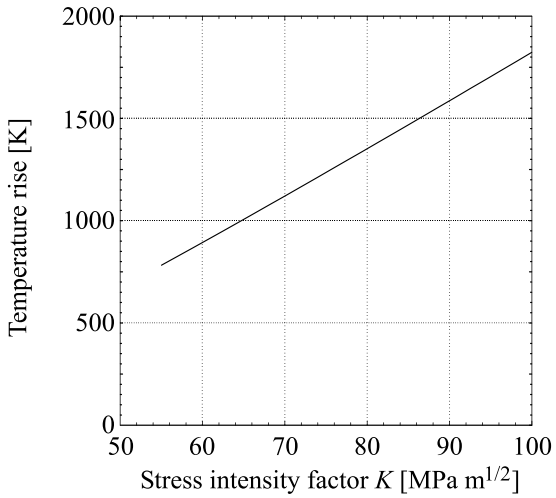

FIGURE 6.2–5 Temperature rise for a running Dugdale crack as a function of the stress intensity factor K (for a Ti-alloy) at constant crack velocity $0.2a_1$.

creases upon increasing temperature. However, usually the toughness *decreases* also with increasing loading rate. The latter effect is commonly attributed to the fact that the effective yield stress is rate dependent whereas the stress level for fracture is essentially independent of the loading rate. Consequently, the loading rate itself and the local temperature rise at the crack tip with increasing loading rate have opposing effects on the toughness.

At first sight, one may think that only at high loading rates the stress intensity factor becomes independent of the rate of loading. It means that we may speculate about the existence of a critical loading rate above which the critical stress intensity factor is not a function of the loading rate anymore. Only in that situation the temperature rise would become the determining factor and an increase of the toughness would be expected at strain rates beyond this critical loading rate[6]. If the strain-rate sensitivity is small, for instance in a Ti-alloy, this critical loading rate effect is probably quite small and an effect of the local temperature rise on the increase in toughness is already expected at lower loading rates. In addition, with increasing local temperature the term $\rho c_P k$ decreases and therefore the temperature rise of equation (6.2−10) becomes a lower bound.

Beside thermal dissipation by crack propagation, there may also exist cooling ahead of the crack tip due to thermo-elastic effects. Assuming that all materials properties stay linear for small stress and temperature changes, the entropy change can be written as[9]

$$\Delta S = \alpha_{ij}\tau_{ij} + \frac{C_\tau}{T}\Delta T \qquad (6.2\text{–}11)$$

where α_{ij} represent the thermal expansion coefficient and C_τ the specific heat under constant stress conditions. If the entropy of an elastic solid is supposed to remain constant, the cooling ahead of the crack can easily be calculated under the assumption that for an isotropic material the specific heat at constant stress is about equal to the specific heat at constant pressure. In figure 6.2–6 the maximum cooling at the crack plane is displayed for various materials as a function of the distance to the crack. The predicted thermo-elastic cooling effect appears to be of minor importance which is in agreement with experiments on metallic glasses[10]. Similarly the cooling in front of a moving edge dislocation is also of the order of one degree.

§6.3 FRACTURE DYNAMICS AND DISCRETE DISLOCATION PLASTICITY

With the approach of Discrete Dislocation Plasticity it is possible to scrutinise to a greater depth the two opposing effects in crack propagation: on the one hand the loading the loading rate and on the other the temperature rise at the crack tip. The

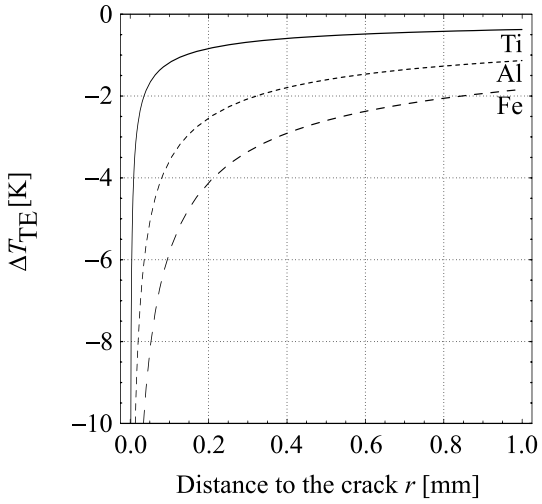

Figure 6.2–6 Thermo-elastic cooling ΔT_{TE} ahead of a crack (Ti, Al, Fe) as a function of the distance r to the crack.

following section is an outlook to future research. Firstly, because dislocations represent discontinuities in displacement, they can also describe a macroscopic crack, at least in a mathematical sense. Furthermore, dislocations facilitate crack opening and plastic relaxation effects. Therefore, the dislocation can be considered not only as a singular dogsbody of the mechanical stress, but also as the basic building block of a crack.

Eshelby, Frank and Nabarro introduced the idea that a crack can be thought of as an array of discrete co-planar and parallel dislocations along the crack plane[11]. However, a much simpler method (in a numerical sense), first suggested by Leibfried[12], is to make a continuum approximation right from the beginning. Instead of dealing with a coplanar row of *discrete* dislocations, it is supposed that the crack plane contains a dislocation density *smeared out* over the crack plane (for dislocation-based fracture mechanics we refer to the recently published text by Weertman[13]). The stress field of a crack running from $-a$ to a can then simply be related to the stress fields of *individual* dislocations and via the dislocation distribution $B(x_1)$ on the crack plane ($x_2 = 0$) by integration

$$\sigma_{ij}^{\text{crack}}(x_1, x_2) = \int_{-a}^{a} B(x_1')\sigma_{ij}^{\text{dis}}(x_1 - x_1', x_2)\mathrm{d}x_1' . \tag{6.3–1}$$

The boundary-value problem of a crack occupying $|x_1| < a$ with $-\infty < x_3 < \infty$ and subjected to either tensile or shear stresses turns out to be equivalent to a *double pile-up* of either edge or screw dislocations in the region $-a < x_1 < a$ caused by a dislocation source at $x_1 = 0$. Components of the stress show a square-root singularity close to the crack tip at $x_1 = \pm a$, $x_2 = 0$. This description is valid for a Griffith crack.

However, it is quite clear that close to the crack tip the stresses are above the yield stress of the material. Plastic flow due to dislocations around the crack-tip region continues until the stress singularity is removed, either by the stresses of the dislocations created during plastic flow, or by blunting of the crack tip due to the emission of dislocations. Mathematically, the pile-up of dislocations produces an infinite stress at the crack tip. Mathematically, this unrealistic result can be avoided by abandoning linear continuum mechanics in the tip region[14]. In terms of dislocation theory, the non-linearity can be dealt with quite simply by allowing some of the leading dislocations in the pile-up to leak away forward into the material ahead of the crack. This is known as the Bilby-Cottrell-Swinden (BCS)-description[15]. In the latter, plastic relaxation is introduced at the crack tip in the region $-c < x_1 < -a$ and $a < x_1 < c$. The relaxation is restricted to the crack plane and to stresses below τ_{YIELD}, the macroscopic yield stress of the material. In fact, the square-root singularity is now replaced by a logarithmic singularity, which is too weak to give rise to a strong stress concentration. The main advantage of the BCS-approach is that it justifies the empirical Orowan-Irwin modification to the Griffith equation. The modification consists of replacing the surface free energy by an *effective* surface energy that includes plasticity in ductile materials. In addition, this model allows for relaxation at the crack tip to be visualised in terms of dislocations moving away from a tip against a resistive stress.

By placing a discrete dislocation in the neighbourhood of a crack, the stress fields of the induced dislocation distribution give rise to stress intensity factors at the crack tip. These factors differ from those belonging to the "classical" crack. Rice and Thomson[16] obtained the stress intensity factors when a discrete dislocation with arbitrary Burgers vector is positioned close to the crack, whereas Weertman[17] gave a general solution of a dislocation placed at arbitrary position. Both solutions refer to a stationary crack. Roberts[18] and others have pursued this line of thinking somewhat further by allowing for multiple dislocations and their motion.

With reference to our own analysis in section 6.2, the 'static' stress intensity factor may depend intricately and subtly on pre-existing dislocations rather than on dislocations nucleated and emitted at the crack tip. It is clear that pre-existing dislocations introduce a new *K'*-field, and depending on the sign of the Burgers vectors these dislocations may either shield or anti-shield the externally applied stress field described solely by *K*. The pre-existing dislocations may multiply and while being attracted to the crack (depending on their Burgers vector), they may cause crack opening displacements. The absorbed Burgers vectors create steps and ledges on the crack plane. The anti-shielding dislocations, which in front of the crack exert an attractive force to the crack, may actually orient in the form of pile-ups from a (Frank-Read) source of length *L* in front of the crack. Actually, this pile-up itself may even generate a microcrack in front of the macrocrack. In that case, the critical stress intensity factor will become proportional to the square root of the distance *L*. In other words, the critical energy release rate for fracture may

become much larger than what one would expect from the length of the crack alone.

To unravel the basic concepts for *dynamic* crack propagation, the DDP-approach may prove itself particularly useful. Only recently a discrete analysis of mode-I crack growth was carried out[19]. There, the fracture properties of a material are based on a cohesive surface constitutive equation and plastic flow occurred by a collective motion of discrete dislocations. From this analysis, it is interesting to note that the fracture behaviour depends very sensitively on the density of pre-existing dislocation sources around the crack. At a low density, only isolated dislocations are generated, leading to brittle failure. At a high density of dislocation sources, a continuous crack tip blunting without crack propagation is observed.

Certainly, when one considers fracture at high strain rate deformation, the dynamics should be properly incorporated. The analysis should *not* be solely based on a stationary crack that emits dislocations, as is usually done in literature. It is feasible that a stationary crack may emit dislocations, whereas a fast moving crack will only nucleate dislocations which are not moving at a velocity high enough to escape from the stress field of the moving crack. In such a situation, although dislocations are nucleated indeed they will not necessarily contribute to a relaxation of the (cleavage) fracture stress. The intrinsically *ductile* failure under stationary conditions may still exhibit a *brittle* failure under dynamic conditions. Indeed, recent results of DDP simulations[20] do suggest this, even though these calculations did not yet include full dynamic, i.e. inertia effects.

Using a relatively simple model of the type used by Roberts, Gumbsch[21] has recently explored some of these issues, again under quasi-static conditions and ignoring dissipative temperature changes. He also confirmed the above-mentioned sensitivity to pre-existing dislocations and the competition between dislocation mobility and nucleation. Although these seem to be all-important aspects of dynamic fracture, to the best of our knowledge there are only a few attempts known in the literature to tackle this question[22] but even so not at the level of dislocations. In principle the DDP-approach, including the local temperature effects as delineated in this thesis, can be explored further to elucidate these fundamental problems in dynamic fracture mechanics at high strain rate deformations.

§6.4 LITERATURE

1. GILLIS P.P., KRATOCHVIL J., *Dislocation acceleration*, Phil. Mag. **21** (1970) 425.
2. DE ANDRADE U.R., MEYERS M.A., VECCHIO K.S., CHOKSHI A.H., *Dynamic recrystallization in high-strain, high-strain-rate plastic deformation of Copper*, Acta Met. et Mat. **42**, (1994), 3183.
3. JOHNSON G.R., HOEGFELDT J.M., LINDHOLM U.S., NAGG A., ASME J. Eng. Mater. Tech. **105** (1983), 42.
4. Coffey C.S., *Shear band formation and localised heating by rapidly moving dislocations*, Inst, Phys. Conf. Ser. No. **70** (1984), 519.
5. CARSLAW H.S., JÄGER J.C., *Conduction of heat in solids* (2nd ed.), Oxford Clarendon Press (1959).
6. RICE J., J. Appl. Mech. **35** (1968), 379.
7. DUGDALE D.C., J. Mech. Phys. Sol. **8** (1960), 100.
8. RICE J., LEVY N., in *Physics of strength and plasticity*, (ed. ARGON A.), MIT Press (1969), 277.
9. NYE J.F., *Physical properties of crystals*, Oxford press, Oxford (1969), 176.
10. FLORES K.M., DAUSKARDT R.H., J. Mater. Res. **14** (1999), 638.
11. ESHELBY J.D., F.C. FRANK F.C, NABARRO F.R.N., *The equilibrium of linear arrays of dislocations*, Phil. Mag. **42** (1951), 351.
12. LEIBFRIED G., *Verteilung von Verzetzungen im statischen Gleichgewicht*, Z. Phys. **130** (1951), 214.
13. WEERTMAN J., *Dislocation based fracture mechanics*, World Scientific, Singapore (1996).
14. BARENBLATT G.I., Adv. Appl. Mech. **7** (1962), 55.
15. BILBY B.A., COTRELL A.H., SWINDEN K., *The spread of plastic yield from a notch*, Proc. Roy. Soc. **A272** (1963), 304.
16. RICE J.R., THOMSON R., *Ductile versus brittle behaviour of crystals*, Phil. Mag. **29** (1974), 73.
17. WEERTMAN J., Int. J. Fracture **26** (1984), 31.
18. ROBERTS S.G., *Modelling the brittle to ductile transition in single crystals*, in in KIRCHNER H.O., KUBIN L.P., PONTIKIS V. (eds.), *Computer simulation in materials science: nano/meso/macroscopic space & time scales*, NATO ASI Series **E308**, Kluwer Dordrecht (1996), 409.
19. CLEVERINGA H.H.M., VAN DER GIESSEN E., J. Mech. Physics of Solids (in press).
20. CLEVERINGA H.H.M, VAN DER GIESSEN E., NEEDLEMAN A., Mat. Sci. and Engineering **A** (in press).
21. GUMBSCH P., GAO H., *Dislocations faster than the speed of sound*, Science 283 (1999), 965.
22. FREUND L.B., *Dynamic fracture mechanics*, Cambridge University Press, London (1993).